Prateek C. Gowda
Department of Biomedical Engineering,
Johns Hopkins University,
1800 Orleans Street,
Sheikh Zayed Tower Ste 7203,
Baltimore, MD 21218
e-mail: pgowda1@jhmi.edu

Victoria X. Chen
Department of Biomedical Engineering,
Johns Hopkins University,
3400 N Charles Street,
Baltimore, MD 21218
e-mail: vchen19@jhu.edu

Miguel C. Sobral
Department of Biomedical Engineering,
Johns Hopkins University,
3400 N Charles Street,
Baltimore, MD 21218
e-mail: miguelsobral98@gmail.com

Taylor L. Bobrow
Department of Biomedical Engineering,
Johns Hopkins University,
733 N Broadway, Traylor 606,
Baltimore, MD 21218
e-mail: tbobrow1@jhmi.edu

Tatiana Gelaf Romer
Department of Biomedical Engineering,
Johns Hopkins University,
3400 N Charles Street,
Baltimore, MD 21218
e-mail: tgelafr1@alumni.jh.edu

Anil K. Palepu
Department of Biomedical Engineering,
Johns Hopkins University,
3400 N Charles Street,
Baltimore, MD 21218
e-mail: anilpalepu@gmail.com

Joanna Y. Guo
Department of Biomedical Engineering,
Johns Hopkins University,
3400 N Charles Street,
Baltimore, MD 21218
e-mail: jguo44@alumni.jh.edu

Dohyung J. Kim
Department of Biomedical Engineering,
Johns Hopkins University,
3400 N Charles Street,
Baltimore, MD 21218
e-mail: dkim165@alumni.jh.edu

Andrew S. Tsai
Department of Biomedical Engineering,
Johns Hopkins University,
3400 N Charles Street,
Baltimore, MD 21218
e-mail: atsai11@alumni.jh.edu

Establishing a Quantitative Endpoint for Transarterial Embolization From Real-Time Pressure Measurements

Transarterial embolization (TAE) is a standard-of-care treatment for tumors in which embolic particles are locally injected via a catheter to occlude blood flow and induce ischemia in the target tissue. Physicians currently rely on subjective visual cues from fluoroscopy in order to determine the procedural endpoint relative to the injection site. This contributes to highly variable treatment outcomes, including the accumulation of embolic particles in healthy tissue, called off-target embolization. To address this concern, we describe a novel, multilumen catheter that 1) measures real-time pressure upstream of the tumor site during TAE injection; and 2) associates that measurement with the volume of embolic particles injected. Using an in vitro silicon vascular model, we characterize the relationship between blood flow, intravascular pressure, and injection pressure. Furthermore, we identify a predictive pressure curve based on the volume of embolic particles injected. This approach has the potential to standardize and optimize TAE, reducing the likelihood of incomplete or off-target embolization, and improving patient outcomes. [DOI: 10.1115/1.4049056]

Manuscript received June 4, 2020; final manuscript received October 21, 2020; published online December 18, 2020. Assoc. Editor: Yaling Liu.

Steven Chen
Department of Biomedical Engineering,
Johns Hopkins University,
3400 N Charles Street,
Baltimore, MD 21218
e-mail: schen207@gmail.com

Clifford R. Weiss[1]
Department of Radiology and
Radiologic Science,
The Johns Hopkins University
School of Medicine,
1800 Orleans Street,
Sheikh Zayed Tower Ste 7203,
Baltimore, MD 21287
e-mail: cweiss@jhmi.edu

Nicholas J. Durr
Department of Biomedical Engineering,
Johns Hopkins University,
3400 N Charles Street,
Baltimore, MD 21218
e-mail: ndurr@jhu.edu

Introduction

Hepatocellular carcinoma (HCC) is the most common primary malignant disease of the liver and the third leading cause of cancer deaths worldwide, accounting for 600,000 deaths globally each year [1,2]. 85% of HCC cases are diagnosed at an advanced stage at which the tumor cannot be surgically resected [1,2]. Transarterial embolization (TAE) therapy is currently the primary alternative to surgery. TAE involves deploying a microcatheter to transvascularly inject drug and/or embolic agents at the tumor site [3]. This procedure induces ischemic necrosis of the tumor by restricting blood flow. TAE was established as a standard of care for intermediate/late-stage HCC in 2006 and it is currently the primary treatment modality for nonresectable cases [4]. Still, there are currently no objective techniques to determine the optimal endpoint for the procedure, resulting in variable tumor responses [1,5]. While *under-embolization* can result in inadequate management of the targeted tumor, *over-embolization* can result in off-target embolic tissue delivery, which increases liver toxicity and expression of angiogenic growth factors. This is associated with a greater rate of local recurrence and reduced survival [1,5].

Digital subtraction angiography (DSA) is the primary method for guiding TAE [1]. The typical metric used by interventional radiologists is to count "beats of stasis" by visualizing the number of heartbeats it takes for a particle/contrast mixture to wash away under DSA. A subjective angiographic chemoembolization endpoint scale attempts to standardize the nomenclature of DSA endpoints for TAE [5]. However, visual cues are subjective and not indicative of the physiological endpoint of the procedure, as evident in the inconsistent outcomes associated with TAE (reported tumor responses range from 15% to 85%) [3]. In fact, numerous studies have found that angiographic endpoints of TAE vary widely, and that interventional radiologists have only moderate reproducibility in classifying these endpoints when using subjective angiographic criteria [6].

The current standard of care has significant limitations. One of the primary causes of off-target embolization is reflux of embolic agents back along the catheter during delivery [7], which has been attributed to high injection pressures during the embolization phase [3]. Since standard microcatheters rely on forward blood flow to move the embolic agent into the tumor and on systolic pressure as the packing force, if the injection pressure exceeds blood pressure, the blood flow can be reversed [3]. This typically results in off-target embolization [3]. The frequency of major complications for patients undergoing TAE is 9.1% per procedure, and off-target embolization accounts for 33% of these major complications [7,8].

Antireflux catheter systems attempt to prevent off-target embolization by physically occluding proximal blood vessels. In doing so, the catheter creates a low-pressure environment for the injection of beads, reportedly increasing on-target embolization [9]. However, these catheters inherently block forward blood flow and distort visual angiographic cues that physicians rely on. Antireflux systems cause a significantly increased rate of over-embolization relative to that of standard microcatheters [4].

The technology presented in this paper establishes a novel quantitative method for interventional radiologists to monitor the extent to which a target tumor has been embolized in real-time, measured as the reduction of blood flow to the tumor. The proposed device is composed of a catheter to deliver the embolic agent as well as a pressure sensor to monitor the extent of occlusion. By continually measuring intravascular pressure, this device allows for 1) consistent, objective determination of a clinically relevant procedural endpoint; and 2) prevention of anterograde reflux and off-target embolization.

Design Requirements

To identify the critical design constraints for our proposed solution, input was gathered from 25 clinical stakeholders, including interventional radiologists and experts of adjacent medical technology products. These interviews, along with a thorough literature review of the space, yielded the following design requirements:

(1) Quantifiable and reproducible determination of the embolization endpoint – The solution should indicate an optimal endpoint to the procedure that physicians can aim for to promote consistent outcomes. This endpoint must accurately reflect complete embolization and be precisely repeatable.

[1]Corresponding author.

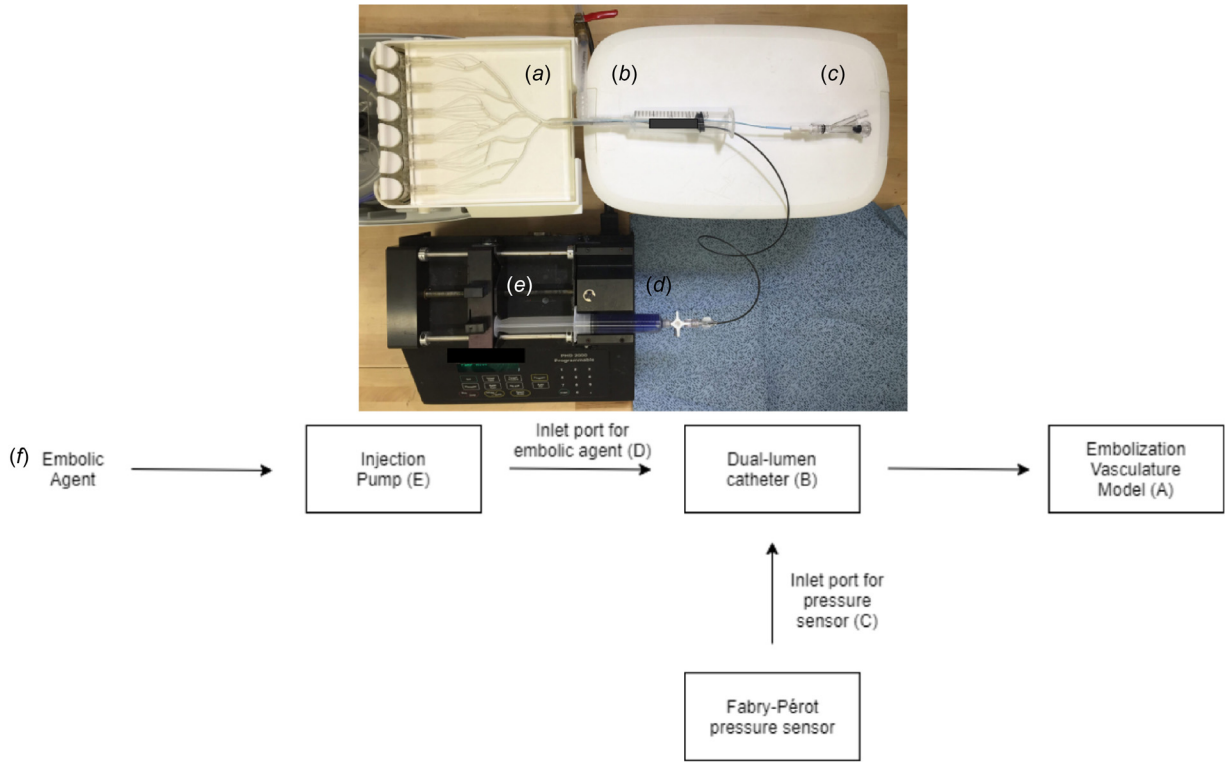

Fig. 1 Image of testing model. (*a*) In vitro embolization vasculature model. (*b*) Prototype of a dual-lumen catheter using a syringe functioning as a hemostasis valve. One lumen (black) serves as a conduit for bead delivery, while the other lumen (blue) houses a Fabry-Pérot (FP) pressure sensor. (*c*) Prototype inlet port for the FP pressure sensor. (*d*) Prototype inlet port for embolic beads and contrast. (*e*) Programmable injection pump for controlled pressure injection of embolic agents. (*f*) Flow-chart of the system consisting of components A-E.

(2) Continuous measurement of vessel occlusion – Vessel occlusion must be measured continually in real-time in order for physicians to assess the extent to which the tumor vasculature is embolized and determine the endpoint.
(3) Integrable into physician workflow – Use of the device must be procedurally similar to the current standard of care to promote physician adoption and integration with other clinical protocols. The device must also be trackable along the guidewire to access deep hepatic sites.
(4) Does not obstruct forward flow – To minimize the risk of over-embolization and preserve visual cues under DSA, the device must not obstruct forward flow and constrain the natural hemodynamics of the system.
(5) Compatible with anatomical dimensions – The solution must work in the microvasculature environment in which TAE is performed. In the case of liver tumor embolization, the typical outer diameter of a microcatheter used to deliver embolic agents is 2.9 Fr (0.97 mm) [10]; the size of embolic particles varies between 30 and 700 μm [11]; and the inner diameter of branching arterioles in the microvascular bed around the tumor is typically 18–25 μm [10].

Concept and Prototype Development

The prototype in this study aims to 1) measure real-time pressure in and around the tumor vasculature; and 2) associate pressure changes with the degree of vessel occlusion, allowing for prevention of retrograde flow and off-target embolization, as well as ensuring complete embolization of the tumor. Previous research suggests that these aims are feasible: measuring changes in hepatic artery pressures has been achieved endoscopically [11]; pressure distal to the tumor is known to increase significantly after chemoembolization [11]; and the pressure drop due to the deployment of an antireflux catheter tip has been shown to correlate with vessel occlusion in complex in vitro and computational models [10].

We present a dual-lumen catheter in which one lumen is dedicated to the delivery of embolic particles, and the other lumen houses a Fabry-Pérot (FP) fiber optic pressure sensor (FOP-M260 by Fiso Technologies, Quebec City, Quebec, Canada) (Fig. 1). The two catheters are threaded through holes in a rubber stopper placed in a syringe, which acts as a hemostasis valve on the proximal end of the device. The FP pressure sensor is waterproof, scalable to the dimensions required for clinical use (1 Fr [0.33 mm] in diameter), and provides continuous measurements over physiologically relevant pressure ranges with the required sensitivity (-300 to 300 mmHg with a sensitivity of $+0.3$ mmHg [-4.00×10^4 to 4.00×10^4 Pa with a sensitivity of $+40$ Pa], and a 30 Hz sampling rate). The catheter material is a braided nylon tube covered with a polytetrafluoroethylene film. The catheter is trackable over the length of a guidewire, which is placed at the desired location of embolization prior to the addition of the prototype.

Testing Methods

To assess the functionality of our prototype, we used a commercial vascular flow simulator (LC Bead M1 Vascular Flow Simulator, Boston Scientific, Marlborough, MA) to simulate the use of the catheter in a hepatic cancer site. This liver vascular model (Fig. 2) included a 1 L reservoir, vascular tree, and 25 mm diameter stainless-steel mesh filters (37 μm opening) that simulate individually embolizable vascular beds. The model received a constant, pressure-controlled flow of water at 100 mmHg to simulate the gauge pressure of physiological blood, and to create a closed-loop flow system. Water was used to simulate blood because blood viscosity is comparable to that of water at the arteriole level. This assumption was derived from the Fahraeus-Lindqvist effect [12]. The following experiments were performed

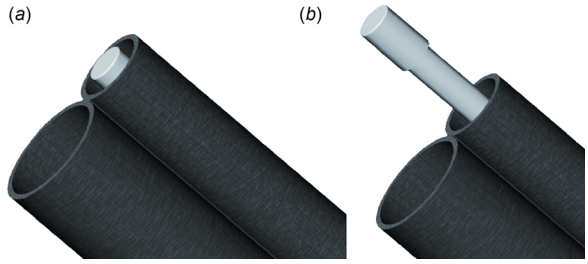

Fig. 2 Distal end catheter design. The catheter is composed of two lumens. The larger lumen (3 Fr [1.00 mm] outer diameter [OD]) is an outlet for embolic particles, injected proximally through a syringe. The guidewire is tracked over the larger lumen when navigating to the desired vasculature location. The smaller lumen (2 Fr [0.66 mm] OD) houses a Fabry-Pérot (FP) sensor (1 Fr [0.33 mm] OD), which measures the pressure at the sensor tip in real-time close to the point of embolic release. Both exploded (*a*) and assembled (*b*) views are shown.

with the branch of vasculature shown in Fig. 3. One branch of the phantom model was embolized to allow for more precise measurement of reflux.

Pressure Versus Volume of Injected Beads. The first protocol characterized the relationship between the pressure reading from the prototype and outflow of the model with the volume of beads injected through the catheter. After placing the catheter at the ingress of the vasculature phantom, tris-acryl gelatin embolic agents (EmboSphere 100–300 μm, Merit Medical, South Jordan, UT) were thoroughly mixed and suspended (20:1 dilution in a physiological saline solution), and injected in increments of 0.5 mL, providing an approximate 1 min delay to ensure flow stasis. Pressure changes were measured in real-time at the ingress of the model, directly adjacent to the catheter, using the fiber optic pressure sensor integrated into our prototype. To quantify the reduction in flow through the model at each injection stage, we measured the outflow rate captured in a graduated cylinder, the volume of the output liquid over a 5 s interval.

Injection Pressure Versus Off-Target Embolization. The second protocol investigated the relationship between injection pressure versus off-target embolization over time. For each iteration of testing, we placed the catheter prototype at a fixed position in the vasculature model, and injected a different amount of embolic agent (0, 1, 2, 3, 4, 4.25, 4.5, 4.75, 5, and 6 mL of bead solution). At each quantity of beads injected, corroborated by measuring the outflow rate from the vasculature model, we injected a 1 mL bolus of water and red Allura Red AC dye at five different injection pressures (13.3, 53.2, 119.8, 213.0, and 332.7 Pa). Videos were recorded of each injection at each volume of bead solution. Our data is presented as on-target and off-target absorption values, which are directly measured from the video frames. The on-target and off-target regions of interest were manually segmented using the MATLAB ROI-Based Processing function in the MATLAB Image Processing Toolbox (Mathworks, Natick, MA). The on-target region was defined as the vasculature downstream of the catheter where the injected beads would ideally settle for the most targeted and effective treatment. The off-target region was defined as the vasculature upstream of the catheter tip. Injected beads would only settle in the off-target region if reflux were to occur, reducing the efficacy of treatment. The on-target and off-target regions of interest were manually segmented and kept constant for all videos.

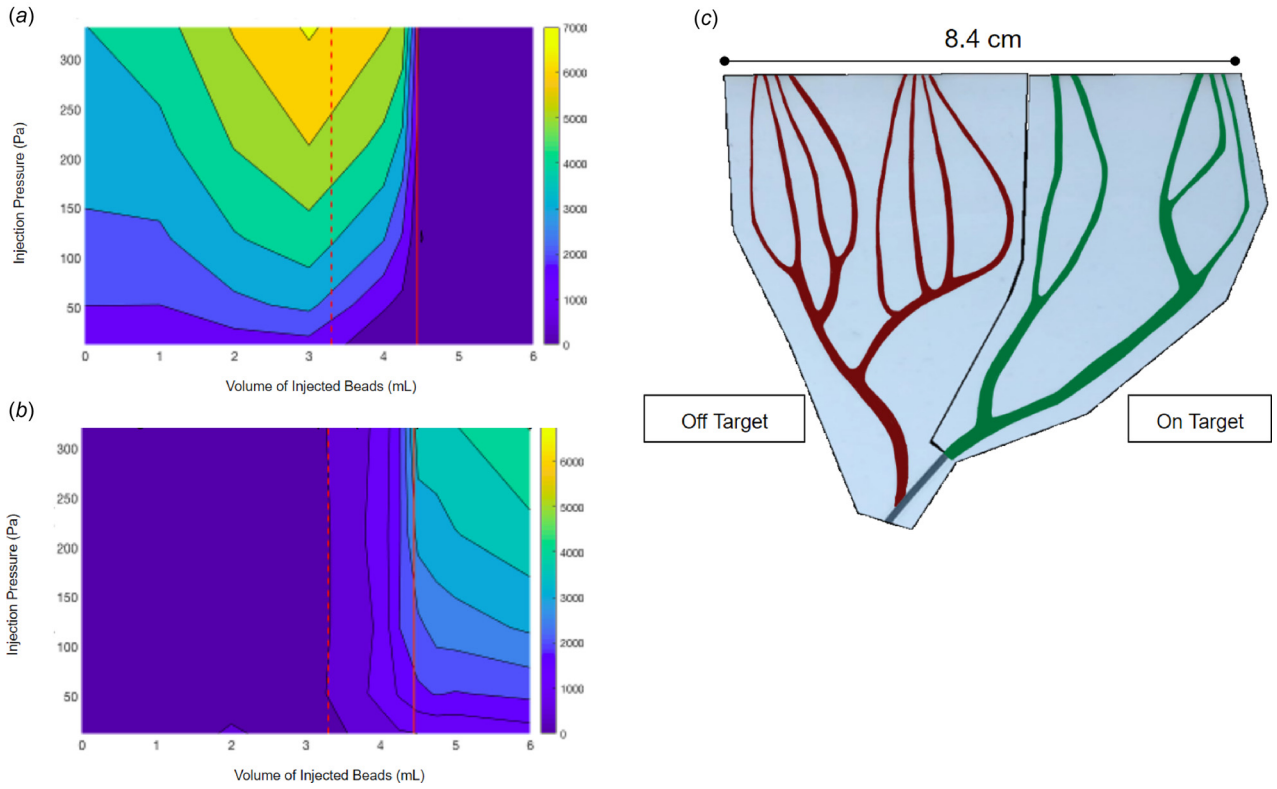

Fig. 3 Left: On-Target Vessel Maximum Absorption (Redness) versus Volume of Injected Beads and Injection Pressure (*a*) and Off-Target Vessel Maximum Absorption (Redness) versus Volume of Injected Beads and Injection Pressure (*b*). The dashed red line marks the start of off-target embolization, and the solid red line marks the end of on-target embolization, when maximum embolization occurs. The absorption is measured in arbitrary relative units. (*c*) Image analysis for the quantification of reflux. Absorption of red hues were measured in the on-target (green tracing) and off-target regions (red tracing) at different injection pressures, with the catheter placed directly leading to the target region.

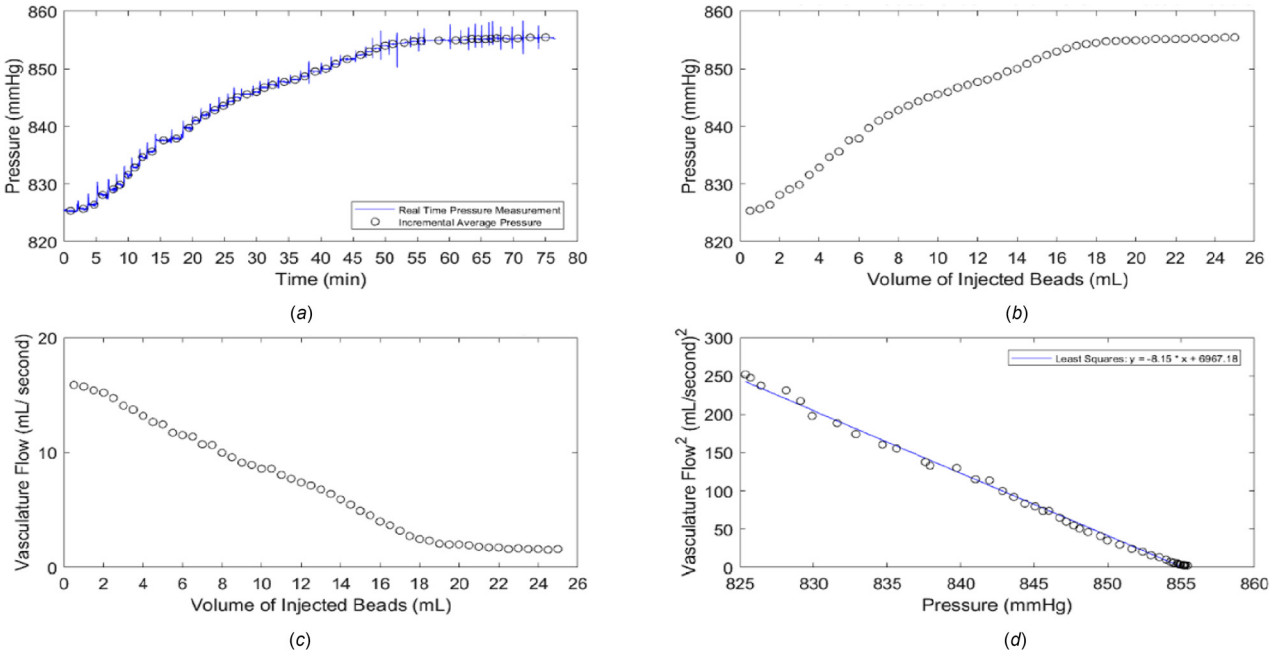

Fig. 4 Data from the pressure and output flow versus volume of beads injected. Shown are pressure readings over time as embolic agents are injected under a constant input pressure of 53.2 Pa (*a*), average pressure at each volume of beads injected (*b*), average flow at each volume of beads injected (*c*), and pressure as a function of flow (*d*). In plot (*a*), each data point is an average of the 100 data points around it. This windowing acts as a low-pass filter to reduce noise in the data. In plot (*a*), the upward spikes indicate instances of the 0.5 mL embolic agent injections. The black circles indicate the average pressure value for a given volume of embolic agents injected. In plot (*d*), a linear regression line is fit to the data. Specifically, we have related pressure to the square of velocity, as supported by Bernoulli's equation.

Results

Pressure Versus Volume of Injected Beads. A stepwise increase in pressure was noted for every 0.5 mL of embolic agents that was injected until a plateau was reached. Once this plateau was reached, repeated injections of embolic agents did not change the pressure. An exponential relationship was observed between pressure and volume of injected beads (Fig. 4(*b*)). In Fig. 4(*c*), the relationship between flow and volume of beads appeared linear until the flow plateaued at 18 mL of injected beads. A quadratic relationship between pressure and rate of flow of liquid through the vasculature was found, as indicated with a linear coefficient of determination of 0.996 between pressure and squared flow (Fig. 4(*d*)).

Injection Pressure Versus Off-Target Embolization. In both on-target and off-target regions, increased injection pressure resulted in a higher concentration of colored contrast in the respective vessel at each quantity of beads injected (Figs. 3(*a*) and 3(*b*)). Off-target contrast started appearing after approximately 3.3 mL of injected beads (dashed red line), and increased with the quantity of beads injected as expected. In complement, on-target contrast levels began decreasing slightly before off-target contrast started appearing, and on-target contrast ceased to appear after around 4.45 mL of injected beads (solid red line). The region between these two red lines represents the period during which contrast was flowing to both on-target and off-target vessels.

Discussion and Conclusions

This study described a novel quantitative method that could be used by interventional radiologists to monitor the extent of tissue embolization in real-time to reduce the likelihood of incomplete or off-target embolization. A quadratic relationship between blood flow and intravascular pressure was found, consistent with Bernoulli's principle and its application to vascular arterial hemodynamics [13]. In addition, we found that high injection pressure might lead to off-target embolization prior to full embolization. Finally, we observed a predictable pressure curve characteristic of embolization procedures that a physician could use to infer the likelihood of retrograde flow.

Using a realistic liver vasculature simulator, we observed a logistic relationship between pressure measured at the catheter tip and quantity of beads injected into the system, demonstrating that real-time catheter pressure measurements could be used as a surrogate marker for patient-specific vessel occlusion. Our prototype measured the largest change in pressure after the first embolic agent injection, and consecutively smaller changes following subsequent injections, eventually resulting in a pressure plateau. We observed this plateau in pressure using our model (Figs. 4(*a*) and 4(*b*)), which also corresponded with a plateau in outflow (Fig. 4(*d*)). These findings indicated that pressure could be used as a correlative metric of the stoppage of flow during embolization procedures. A near-complete stop to flow indicated complete occlusion of the vessel and therefore effective embolization. Thus, through real-time pressure readings, physicians would know that they had achieved 100% embolization once they saw a plateau in pressure.

The stated design goals are critical to achieving an impactful product. The pressure sensing system did not alter the standard embolization procedure itself, while being able to measure pressure without obstructing flow within a vascular system similar to anatomical dimensions. These key characteristics combined with the data obtained in this study serve as a proof of concept that an embolization endpoint can be achieved with real-time pressure measurement in a manner that is compatible with our stated design goals.

Video analysis of reflux into off-target vessels occurred before maximum embolization was reached in on-target vessels (Fig. 3(*a*)). Furthermore, reflux into off-target vessels demonstrated that increased injection pressure caused increased reflux in off-target vessels, and that reflux tended to increase at constant

injection pressures as the vessel reached complete occlusion (Fig. 3(*b*)). This confirms that there was a range of injection pressures and degrees of embolization (in between the dashed and solid red lines) during which physicians would need to be especially careful to avoid reflux before the embolization endpoint was reached.

In the near term, the relationship between injection pressure and readings on the pressure sensor that we have observed need to be corroborated in an in vivo setting. Furthermore, an experimental protocol allowing for measurement of injection pressure, pressure within the vasculature, and off-target embolization simultaneously must be developed. Doing so will allow the use of pressure readings to alert physicians of the aforementioned range in which reflux can occur before the embolization endpoint is reached, as well as the injection pressures that they should not exceed. It will also allow us to understand the relationship between real-time pressure readings, expected reflux, and vessel occlusion. Further pressure measurements within in vivo and clinical studies may only require a lower fidelity fluid-filled catheter with a pressure transducer located outside the subject. This could serve to reduce prototyping costs and promote reusability of equipment.

Additionally, an increase in spike amplitude was observed as pressure began to plateau (Fig 4(*a*)). It can be hypothesized that this is due to the increased resistance that results from increased embolic agent, but more work needs to be done in future studies to validate this intuition.

In the long term, in order to optimize our catheter design for a microvasculature setting (maximum of 4 Fr [1.33 mm] total diameter), the procedural costs and benefits of double-lumen versus single-lumen catheter designs need to be assessed. Additionally, an automated infusion system should be tested to explore the potential benefits of a titrated infusion over a bolus infusion (the current standard of care), as that may allow a more consistent and controlled distal embolization, and thus a lower risk of reflux. Finally, pressure measurements may serve to provide a predictive value for the endpoint, such that physicians can aim for a predetermined target pressure that would indicate full embolization. A possible solution would be to temporarily and completely obstruct the vessel just distal to the catheter tip, e.g., with an inflated balloon, measure the pressure, then remove the obstruction. The measured "final pressure" would simulate the scenario of a completely occluded vessel, which physicians would then use as a quantitative endpoint for the procedure. Further experimentation in clinical models is required to validate this concept.

It is important to note that we define effective embolization as 100% occlusion of the blood vessel. However, in cases in which the physician would only aim for partial occlusion, we would need a way to determine how much embolic agent is needed to achieve a specified percentage of complete embolization. In other words, we would need a way to define 100% occlusion before embolization actually reaches this stage. Predictive models would need to be developed to obtain these preemptive measurements.

Here, we have demonstrated in vitro proof of concept of a novel, objective approach to allow interventional radiologists to establish a procedural endpoint during TAE therapy to increase therapeutic success.

Acknowledgment

The funders had no role in the study design, data collection and analysis, decision to publish, or preparation of the paper.

Funding Data

- VentureWell E-Teams.
- The Johns Hopkins University Biomedical Engineering Department, Center for Bioengineering Innovation & Design (Funder ID: 10.13039/100007880).

References

[1] Bruix, J., and Sherman, M., 2011, "Management of Hepatocellular Carcinoma: An Update," Hepatology, **53**(3), pp. 1020–1022.

[2] American Cancer Society, 2020, "Key Statistics About Liver Cancer," American Cancer Society, Atlanta, GA, accessed Oct. 20, 2020, https://www.cancer.org/cancer/liver-cancer/about/what-is-key-statistics.html

[3] Allen, M. P., 2018, "Device and Methods for Transvascular Tumor Embolization With Integrated Flow Regulation," US Patent No. US10130762B2.

[4] Tsochatzis, E. A., Germani, G., and Burroughs, A. K., 2010, "Transarterial Chemoembolization, Transarterial Chemotherapy, and Intra-Arterial Chemotherapy for Hepatocellular Carcinoma Treatment," Semin. Oncol., **37**(2), pp. 89–93.

[5] Ahmed, M., 2014, "Image-Guided Tumor Ablation: Standardization of Terminology and Reporting Criteria—a 10-Year Update: Supplement to the Consensus Document," J. Vasc. Interventional Radiology, **25**(11), pp. 1706–1708.

[6] Lewandowski, R. J., Sato, K. T., Atassi, B., Ryu, R. K., Nemcek, A. A., Kulik, L., Geschwind, J., Murthy, R., Rilling, W., Liu, D., Bester, L., Bilbao, J. I., Kennedy, A. S., Omary, R. A., and Salem, R., 2007, "Radioembolization With 90Y Microspheres: Angiographic and Technical Considerations," Cardiovasc. Interventional Radiology, **30**(4), pp. 571–592.

[7] Poggi, G., Emma, P., Riccardi, A., Tonini, S., Montagna, B., Quaretti, P., Tagliaferri, B., Sottotetti, F., Baiardi, P., Pagella, C., Minoia, C., and Bernardo, G., 2010, "Complications of Image-Guided Transcatheter Hepatic Chemoembolization of Primary and Secondary Tumours of the Liver," Anticancer Res., **30**(12), pp. 5159–5164.

[8] Sakamoto, I., Aso, N., Nagaoki, K., Matsuoka, Y., Uetani, M., Ashizawa, K., Iwanaga, S., Mori, M., Morikawa, M., Fukuda, T., Hayashi, K., and Matsunaga, N., 1998, "Complications Associated With Transcatheter Arterial Embolization for Hepatic Tumors," Radiographics, **18**(3), pp. 605–619.

[9] Rose, S. C., Halstead, G. D., and Narsinh, K. H., 2017, "Pressure-Directed Embolization of Hepatic Arteries in a Porcine Model Using a Temporary Occlusion Balloon Microcatheter: Proof of Concept," Cardiovasc. Interventional Radiology, **40**(11), pp. 1769–1776.

[10] Rose, S. C., Kikolski, S. G., Morshedi, M. M., and Narsinh, K. H., 2015, "Feasibility of Intraprocedural Transluminal Hepatic and Femoral Artery Blood Pressure Measurements as an Alternative Embolization Safety Endpoint When Antireflux Devices Are Used During Lobar Chemoembolization," Am. J. Roentgenology, **205**(1), pp. 196–202.

[11] Borowski, A. M., Frangos, A., Mccann, J. W., and Brown, D. B., 2013, "Pressure Wire Assessment of Hemodynamic Alterations After Chemoembolization of Hepatocellular Carcinoma," Academic Radiology, **20**(8), pp. 1037–1040.

[12] Cortinovis, A., Crippa, A., Cavalli, R., Corti, M., and Cattaneo, L., 2006, "Capillary Blood Viscosity in Microcirculation," Clinical Hemorheology Microcirc., **35**(1–2), pp. 183–192.

[13] Šutalo, I. D., Lawrence-Brown, M. M., Liffman, K., and Semmens, J. B., 2016, "Vascular Arterial Haemodynamics," *Oxford Textbook of Vascular Surgery*, Oxford University Press, Oxford, UK, pp. 128–133.